

A Miniaturized MIMO Antenna for C, X, and Ku Band Applications

Ajit K. Singh^{1, *}, Santosh K. Mahto¹, and Rashmi Sinha²

Abstract—A dual-element miniaturized multiple-input-multiple-output (MIMO) antenna with a defected ground plane (DGS) and a tapered microstrip feed line is introduced in this article. It achieves a bandwidth (BW) of 10.8 GHz (7.2–18 GHz), frequency ratio (FR) of 2.5, and average isolation of 15 dB over the entire operating band. The proposed antenna is right hand circularly polarized (RHCP) and achieves an axial ratio of < 3 dB in the frequency band ranging from 7.2 to 8.9 GHz. The performance characteristics of the proposed antenna are analyzed in terms of the envelope correlation coefficient (ECC), mean effective gain (MEG), total active reflection coefficient (TARC), isolation between the ports, and channel capacity loss (CCL), and the values obtained are 0.1607, 9.99 dB, ± 3 dB, -11 dB, -7 dB, 0.20 bits/sec/Hz, respectively. The proposed MIMO antenna is fabricated on an FR-4 dielectric substrate of dimension $10.6 \times 10.3 \times 1.6$ mm³ and has good agreement between simulated and experimental results. The proposed antenna can be used for C, X, and Ku band applications.

1. INTRODUCTION

Wideband antenna system has entranced the modern wireless world with its appealing highlights like multi-band communication, high data rate, high capacity, good resolution, and negligible operational energy. However, the multipath propagation and space impediments degrade the performance of a single-input-single-output (SISO) system. In wireless devices, there is a necessity of miniaturized MIMO antenna configurations, which may achieve low inter-element isolation and ensuing debasement in its performance [1–4]. Different diversity techniques can be used to improve the reliability of transmission links by lessening the multipath fading issue.

Several single element [5–10] and MIMO [11–17] antennas have been reported in the literature for multiple wireless applications. A modified E-shaped patch antenna has been designed with a dimension of $9.4 \times 7.1 \times 0.8$ mm³ [5]. In [6], a dual-band circularly polarised spidron fractal patch antenna has been designed for the Ku band application with FR of 1.16 and dimension of $50 \times 50 \times 1.6$ mm³. A compact dual-band microstrip antenna was proposed with an FR of 1.13 [7]. In [8], a dual-band triple frequency X-shaped patch antenna has been proposed for K and Ku band satellite applications with an FR of 1.14. A low profile, low-cost antenna has been proposed for Ku band applications with an FR of 1.19 and dimension of $9.9 \times 10.1 \times 1.6$ mm³ [9]. In [10], a small size, light weight, dual-band antenna was proposed for satellite applications with an FR of 1.16.

The reliability, robustness, and security of the receiving system improve as the number of antennas with identical spectral characteristics increases at the receiving terminal; however, space is a major concern. Also the effect of mutual coupling increases as the distance between antenna elements decreases, which affects the diversity performance of the MIMO system.

A dual-band MIMO antenna resonating at 7.6 GHz and 14.4 GHz frequencies was proposed with a dimension of $24 \times 20 \times 1.6$ mm³ and an isolation of 20 dB with an ECC of 0.04 [11]. In [12], a compact

Received 2 October 2021, Accepted 2 December 2021, Scheduled 13 December 2021

* Corresponding author: Ajit K. Singh (ajitsingh31393@gmail.com).

¹ Indian Institute of Information Technology, Ranchi, Jharkhand, India. ² National Institute of Technology Jamshedpur, Jharkhand, India.

MIMO antenna designed on a Rogers Duroid 5880 substrate with a frequency ratio of 6.05, ECC of 0.1, and peak gain of 5.3, respectively. An I-shaped defected ground structure MIMO antenna was proposed for 5.8 GHz frequency band with an isolation, dimension, and ECC being 25 dB, $50.54 \times 21.29 \times 1.6 \text{ mm}^3$, and 0.2, respectively [13]. A quad element MIMO antenna was proposed with impedance bandwidth of 8.7 GHz (7.8 GHz – 16.5 GHz). The proposed antenna has a frequency ratio of 2.11 with an isolation of 15 dB [14]. In [15], a compact MIMO antenna was proposed for C and X band applications with a dimension of $17 \times 42 \times 1.6 \text{ mm}^3$ and ECC of 0.015. In [16], a dual port MIMO antenna with high isolation of 25 dB was proposed with a dimension of $16 \times 28 \times 1.6 \text{ mm}^3$ for X band applications. A four-element MIMO antenna with a dimension of $46.7 \times 46.7 \times 1.6 \text{ mm}^3$ was proposed for X band applications. The antenna achieved a circular polarization by using Tai Chi-shaped patches and L-shaped feeds in the frequency band of 9.75–10.41 GHz [17].

This motivated us to design a 1×2 or 2×1 MIMO antenna with good isolation and efficiency as reported in Table 2. The designed antenna has compact volume that includes two radiating elements with good diversity performance. The proposed antenna achieved a good frequency ratio (FR) other than those reported in Table 2, which signifies the wide band characteristics of the antenna.

In this article, a dual-element miniaturized MIMO antenna has a dimension of $10.6 \times 10.3 \times 1.6 \text{ mm}^3$ for frequency ranging 7.2–18 GHz with a frequency ratio of 2.5. Therefore, the proposed antenna design has ample opportunity for a variety of applications such as Downlink Satellite System (DSS: 7.25 GHz–7.75 GHz) interference, in the region-3 spectrum assigned by ITU for fixed satellite services (FSS) which is 12.2 to 12.7 GHz in receiving mode and 14 to 14.5 GHz in transmitting mode. Likewise for radio applications (13.4–14 GHz) and direct broadcast services (DBS), the assigned frequency band is 11.7 to 12.2 GHz in receiver mode and 17.3 to 17.8 GHz in transmitter mode.

2. DESIGN

Figure 1 shows the geometry of proposed MIMO radiator antenna. The antenna is printed on an FR4 substrate having a dielectric constant of 4.4 and loss tangent of 0.02 with a total volume of $10.6 \text{ mm} \times 10.3 \text{ mm} \times 1.6 \text{ mm}$, and the optimized antenna parameters are mentioned in Table 1. The evolution of the proposed antenna is shown in Figure 2.

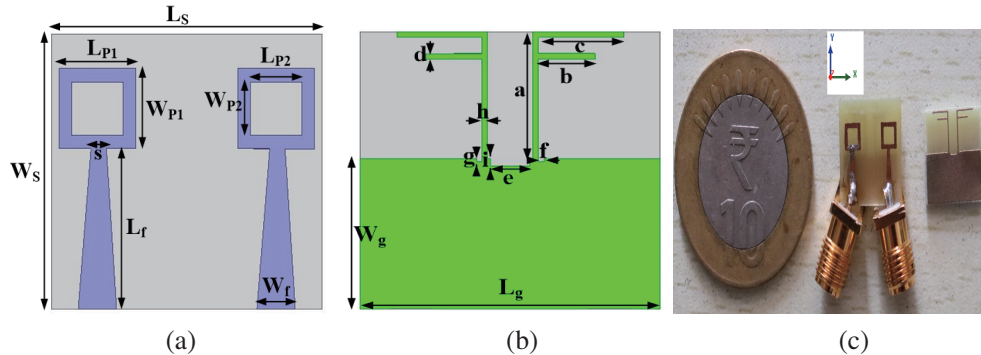


Figure 1. Proposed MIMO antenna. (a) Front view. (b) Back view. (c) Fabricated antenna.

Antenna-1 consists of two $3 \text{ mm} \times 3 \text{ mm}$ square patches and tapered feed, and a pair of F-shaped stubs with unequal arm is inserted on the ground plane as shown in Figure 2(a). It does not provide satisfactory results as shown in Figure 3. Antenna-2 utilizing a similar configuration like Antenna 1 with a rectangular slot and two vertical slots is engraved in the ground plane to improve bandwidth as shown in Figure 2(b) because it adjusts the electromagnetic coupling effect between the patch and the ground plane, and improves its impedance bandwidth with compact size. However, return loss is not improved in the lower frequency range as shown in Figure 3, and also Antenna-1 and Antenna-2 have linear polarization. Antenna-3 utilizes a similar configuration like Antenna 1 and by etching a square slot of dimension $2 \text{ mm} \times 2 \text{ mm}$ inside the patches as shown in Figure 2(c). However, it does not provide circular polarization along with reflection coefficient in the lower frequency range as shown in Figure 3.

Table 1. Optimize dimensions of proposed antenna.

Symbol	Value (mm)	Symbol	Value (mm)	Symbol	Value (mm)
L_S	10.6	W_f	1.5	f	0.2
W_S	10.3	s	0.5	g	0.12
L_{P1}	3	a	5	h	0.2
W_{P1}	3	b	2	i	0.28
L_{P2}	2	c	3	L_g	10.6
W_{P2}	2	d	0.2	W_g	5.6
L_f	6	e	1.4		

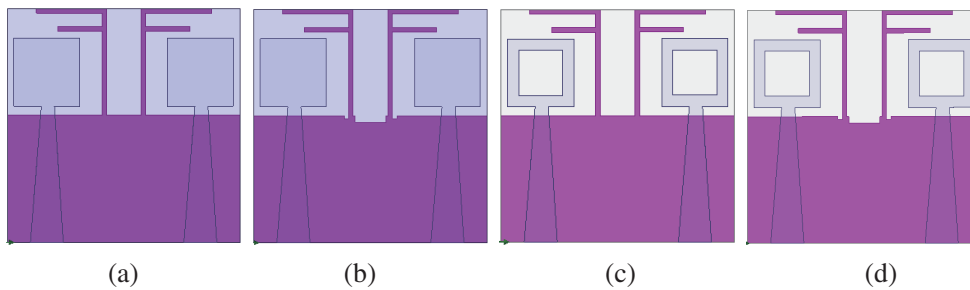


Figure 2. Geometrical configuration of proposed antenna. (a) Antenna-1. (b) Antenna-2. (c) Antenna-3. (d) Antenna-4.

In the proposed MIMO antenna a rectangular slot and two vertical slots are engraved in the ground plane of Antenna 3 as shown in Figure 2(d) to improve the impedance bandwidth from 7.2 GHz to 18 GHz and also by etching a square slot inside the patches to achieve the circular polarization because of advancement of the growth in the lengths of the current path as delineated in Figure 3(a) and Figure 4(b), respectively. The circular polarization is usually influenced because of the coupling capacitance between the patch and the ground plane.

Further, a parametric analysis of the proposed antenna is performed by varying the feed width ($W_f = 1.1-1.5$ mm) and length, ($s = 0.30-0.60$ mm), and return loss is not satisfactory from 8–9 GHz and 7.2–10.5 GHz frequency ranges, respectively as shown in Figure 3(a). The wideband characteristics of the antenna are achieved by considering the feed width $W_f = 1.5$ mm and $s = 0.60$ mm as delineated in Figure 3.

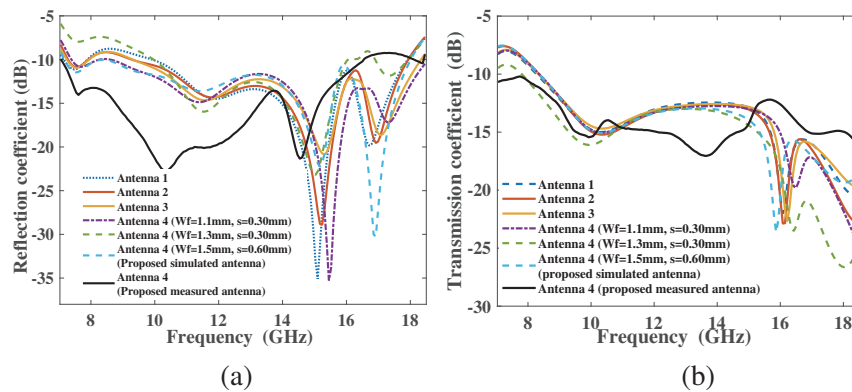


Figure 3. Simulated & measured (a) reflection coefficient (b) transmission coefficient.

3. RESULTS AND DISCUSSION

Measured and simulated reflection and transmission coefficients of the MIMO antenna, as represented in Figures 3(a)–(b) are < -10 dB, -13 dB, respectively, throughout the entire frequency range. However, there is a slight mismatch in simulated and measured results from the 16.8 GHz–17.5 GHz frequency band due to human errors and fabrication tolerances.

Group delay is characterized as the negative derivative of phase of the transfer function against frequency and shown in

$$\tau_g(\omega) = -\frac{d\phi(\omega)}{d\omega} = -\frac{d\phi(f)}{2\pi df} \quad (1)$$

in which $\phi(f)$ and ϕ are the frequency-dependent phase of the radiated signal. If group delay is not same for all the frequency supported by the antenna, then distorted signal will be found which is not expected. From Figure 4(a) we observe that a constant group delay is obtained over the intended BW (7.2–18 GHz), however, a slight deviation of < 0.5 ns from 15.1 to 16 GHz.

Generally, MIMO antennas may have linear polarization (LP) or circular polarization (CP). However, typically the CP is preferred due to its advantages such as the ability to overcome multipath fading, admirable behavior in bad weather conditions, and acceptable mobility. Consequently, the CP produces a considerably high quality of communication service. The operating bandwidth of a CP antenna is defined as a frequency band in which the bandwidth where $|S_{11}| < -10$ dB and that achieves an axial ratio (AR) of < 3 dB. Figure 4(b) presents the axial ratio and RHCP gain graph against the frequency for different antennas. It is apparent from the graph that the MIMO antenna is RHCP with an AR of < 3 dB in a frequency ranging from 7.2 to 8.9 GHz.

Figure 4(c) shows the peak gain and the total efficiency over the entire operating band of the proposed configuration. The antenna achieved an average peak gain and total efficiency 2.21 dBi and 69.8% (-0.90 dB), respectively, as shown in Figure 4(c), which is acceptable for the practical applications.

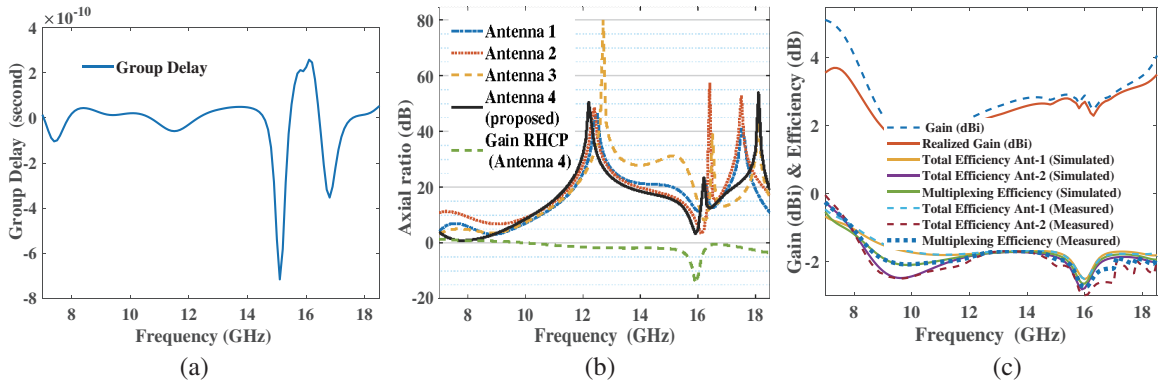


Figure 4. (a) Group delay. (b) Axial ratio. (c) Gain & efficiency.

Figure 5 presents the co- and cross-polarizations of the MIMO antenna at 8 GHz and 12.5 GHz frequencies at y - z and x - z planes. The DGS is designed in such a way that the fundamental radiating mode remains unaffected, and at the same time the fringing orthogonal fields along the H -plane are weakened efficiently leading to better suppression in cross-polarization. At some angles, the level of a cross polar pattern is greater than the co-polar pattern because of the excitation of hybrid mode at higher frequencies.

Figure 6 presents the surface current density of the MIMO antenna at 8 GHz, 12.5 GHz, and 18 GHz frequencies. A low surface current is seen in Ant-2 because Ant-1 is excited at a time and other ports terminated with 50Ω load. Moreover, a strong surface current is induced on Ant-1 and the inverted F-stubs associated in the ground plane. Subsequently, the low isolation between Ant-1 and Ant-2 shows that the proposed decoupling mechanism is important in different antenna applications without impacting the adjoining antenna.

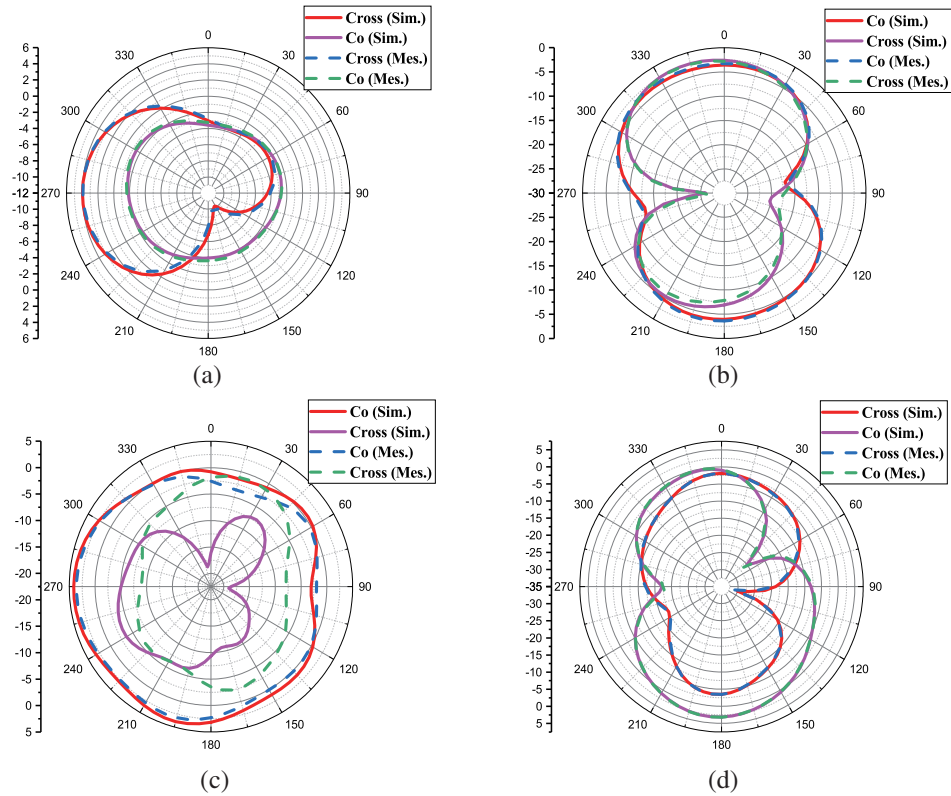


Figure 5. Co & Cross-polarization (a) y - z plane at 8 GHz. (b) x - z plane at 8 GHz. (c) y - z plane at 12.5 GHz. (d) x - z plane at 12.5 GHz.

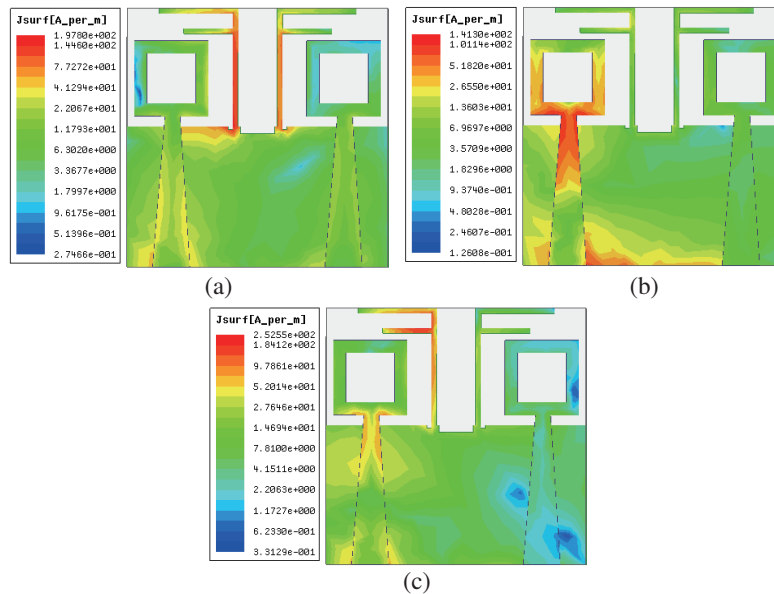


Figure 6. Surface current density (a) 8 GHz, (b) 12.5 GHz, (c) 18 GHz.

The MIMO antenna is fabricated on an FR4 substrate, and the antenna under test is put in an anechoic chamber related to VNA (Vector Network Analyzer) for measurement of antenna traits, shown in Figure 7.

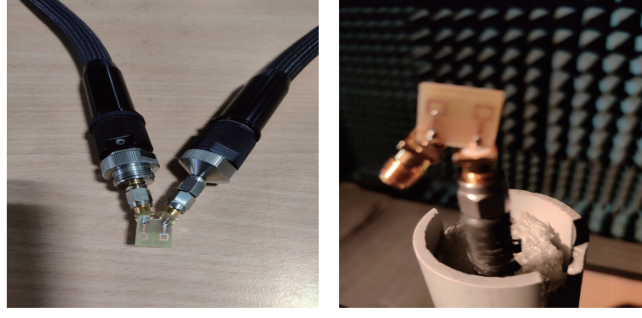


Figure 7. Measurement setup of proposed antenna.

4. MIMO DIVERSITY PERFORMANCE

In order to ensure the compatibility of the designed wideband MIMO antenna, ECC, TARC, MEG, and DG parameters are evaluated and discussed. The amount of correlation between the radiation patterns of MIMO elements is dictated by ECC and determined using (2) [18].

$$ECC = \frac{|S_{11}^* S_{12} + S_{21}^* S_{22}|^2}{(1 - |S_{11}|^2 - |S_{21}|^2)(1 - |S_{22}|^2 - |S_{12}|^2)} \quad (2)$$

$$|\rho_{ij}|_{guaranteed} = |\rho_{ij}| + \sqrt{\left(\frac{1}{\eta_{radi}} - 1\right)\left(\frac{1}{\eta_{radj}} - 1\right)} \quad (3)$$

where,

$$\rho_{ij} = \frac{-S_{ii} S_{ij}^* - S_{ji} S_{jj}^*}{\sqrt{(1 - |S_{ii}|^2 - |S_{ji}|^2)(1 - |S_{jj}|^2 - |S_{ij}|^2)\eta_{radi}\eta_{radj}}} \quad (4)$$

and ECC guaranteed is calculated by,

$$|\rho_{eij}|_{guaranteed} = |\rho_{ij}|_{guaranteed}^2 \quad (5)$$

in which i and j denote ANT-1 and ANT-2, respectively. From Equations (3) and (5), the calculated values of $|\rho_{ij}|_{guaranteed} \leq 0.4009$ and $|\rho_{eij}|_{guaranteed} \leq 0.1607$. These values show the worst case of channel correlation by including the antenna losses.

The value of ECC is zero for an ideal case; however, the practical value is ≤ 0.5 . For lossless condition, ECC is calculated by Equation (2) and shown in Figure 8(a). DG is portrayed as the amount of progress acquired from an array system comparative to a single element and determined as:

$$DG = 10\sqrt{1 - ECC^2} \quad (6)$$

DG should be near 10 dB.

Effective Diversity Gain (EDG) is used to calculate radiation losses in MIMO antenna and determined by Equation (7). The EDG and DG values are equal if the total efficiency (η_{Total}) = 1. The average DG of the MIMO antenna is 9.99 dB while EDG is around 8.2 dB as shown in Figure 8(b).

$$EDG = \eta_{Total} \times DG \quad (7)$$

$$\eta_{Total} = \eta(1 - |S_{11}|^2 - |S_{21}|^2) \quad (8)$$

in which η is the radiation efficiency.

In the case of a dual-element antenna, adjacent antenna components encroach on one another when operating simultaneously. This deteriorates the antenna performance. Subsequently, the performance of MIMO antenna cannot be anticipated by S -parameters only, so TARC is considered to account for this effect. For a two element antenna TARC can be determined as

$$TARC = \sqrt{\frac{(S_{11} + S_{12})^2 + (S_{21} + S_{22})^2}{2}} \quad (9)$$

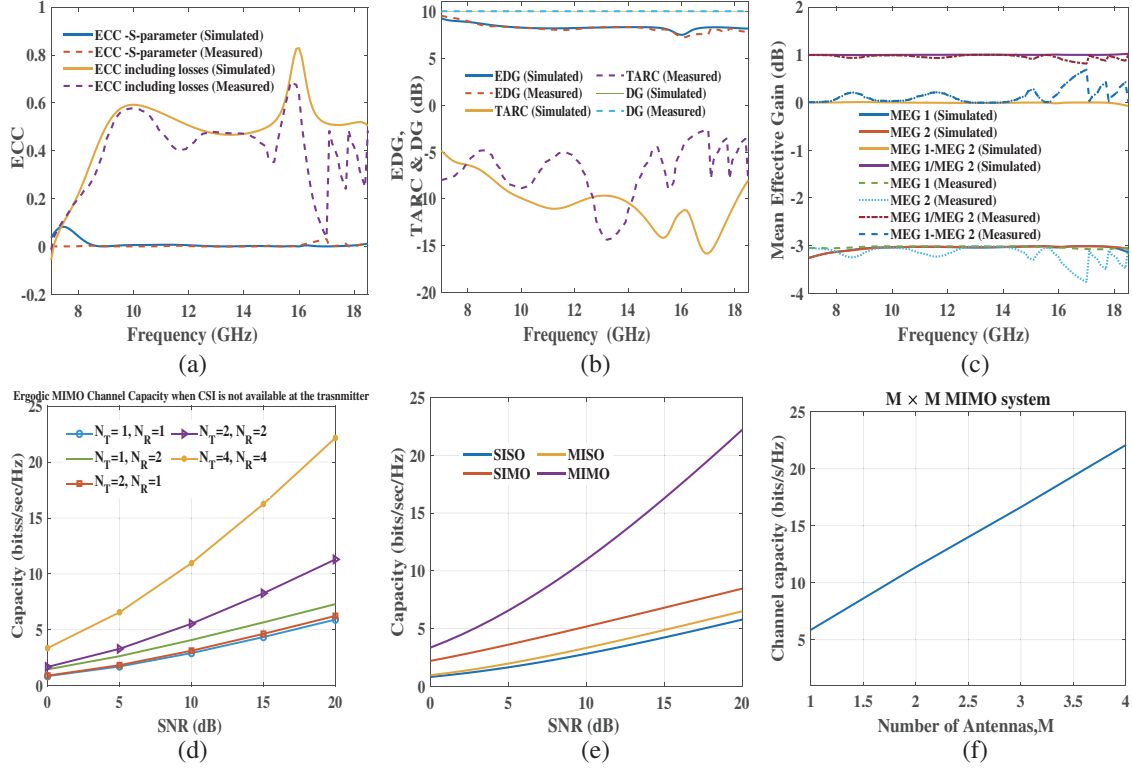


Figure 8. Diversity plot (a) ECC, (b) EDG, TARC,& DG, (c) MEG, (d) Ergodic capacity, (e) Comparative analysis, (f) Capacity v/s no. of antenna elements.

In an ideal case, $TARC < 0$ dB for MIMO antenna. The simulated and experimental TARCs of the structured MIMO antenna are less than -7 dB as depicted in Figure 8(b). In a fading environment, MEG is the proportion of the mean received power to the mean incident power of the antenna. The MEG is assessed for two element using formulas (10) and (11) [19],

$$MEG_i = 0.5 \left[1 - \sum_{j=1}^N |S_{ij}|^2 \right] < -3 \text{ dB} \quad (10)$$

$$MEG_j = 0.5 \left[1 - \sum_{i=1}^N |S_{ij}|^2 \right] < -3 \text{ dB} \quad (11)$$

$$\text{Also, } |MEG_i - MEG_j| < 3 \text{ dB} \quad \& \quad |MEG_i / MEG_j| = \pm 3 \text{ dB} \quad (12)$$

in which i and j denote ANT-1 and ANT-2, respectively. The calculated MEG using S -parameter is depicted in Figure 8(c).

Channel Capacity — The performance of MIMO system is determined using channel capacity which is proportional to bandwidth and signal to noise ratio (SNR). The equal power is given to the transmitting antenna element. The Ergodic MIMO channel capacity for two-element antenna arrays is calculated by using [18]

$$C_{2 \times 2 \text{ MIMO} (Max.)} = n \left(b \left[\log_2 \left[\det \left([I] + \frac{SNR}{n} [H][H^*] \right) \right] \right] \right) \quad (13)$$

where $[I]$ is an $n \times n$ identity matrix. n is the number of antenna array elements, $[H]$ the normalized channel matrix, and $[H^*]$ the transpose conjugate of the channel matrix. SNR is $20 \text{ dB} = 100$ for Rayleigh fading environment.

The correlation matrix is determined by

$$R_{xx}(\gamma) = \gamma [I] + (1 - \gamma) [H][H^*] \quad (14)$$

where γ is the channel correlation coefficient that lies from 0 to $\frac{n}{n-1}$. $\gamma = 0$, means channels are correlated to each other whereas $\gamma = 1$ means channels are uncorrelated. The ergodic capacity of the antenna is shown in Figure 8(d).

The channel capacity of single-input-single-output (SISO), single-input-multiple-output (SIMO), multiple-input-single-output (MISO), and MIMO in terms of SNR for several values of transmitting (N_T) and receiving antennas (N_R) are mentioned in Figure 8(e). It can be seen that capacity of SISO is slow with respect to increasing SNR; however, the capacity of MIMO system is large (almost 3 times the capacity of SISO). The results show that the capacity of MIMO system increases with increasing SNR.

Further, the capacity of MIMO system w.r.t number of antennas is mentioned in Figure 8(f). It shows that capacity grows linearly w.r.t the number of antennas, and channel capacity losses (CCLs) are likewise increased [20].

CCL is shown in Figure 9 and determined by Equation (15) [21].

$$CCL = -\log_2 \det[\beta^R] \quad (15)$$

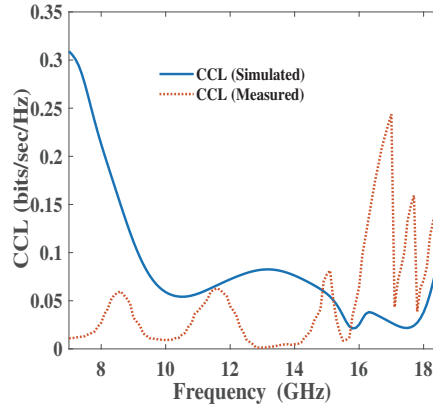


Figure 9. CCL

Table 2. Comparison of proposed MIMO antenna with other proposed antenna.

Ref.	Dimension (mm ³)	Bandwidth (GHz)	FR ($\frac{F_H}{F_L}$)	Isolation (dB)	ECC	Gain (dBi)	Applications
[5]	9.4×7.1×0.8	11.95–14.25	1.19	-	-	5.7–7.2	Ku band
[6]	50 ×50×1.5	11.96–13.93	1.16	-	-	3.7–3.8	Ku band
[7]	5.7×8×1.9	12.72–14.4	1.13	-	-	5–5.5	Ku band
[8]	9.5×8×1.9	15.33–17.61	1.14	-	-	4.8–6.4	satellite applications
[9]	9.9×10.1×1.6	12.07–14.44	1.19	-	-	4.8–7.4	satellite applications
[10]	10×10×1.6	12.38–14.40	1.16	-	-	1.6–4.2	Ku band
[11]	24×20×1.6	7.6,14.4	-	20	0.04	-	X & Ku band
[12]	18×30×0.8	3.21–19.43	6.05	18	0.1	5.33	UWB/X/Ku
[13]	50.54×21.29×1.6	5.56–7.73	-	25	0.2	3.5–6	Short range RADAR
[14]	25×25×1.6	7.8–16.5	2.11	15	0.14	1.02–5.5	X & Ku band
[15]	17×42×1.6	6.6–7.6, 8.3–10	1,1,2	22	0.015	1.7–5	C & X band
[16]	16×28×1.6	2.95–15.65	5.30	25	0.04	1.2–6.8	UWB, X & Ku band
[17]	46.7×46.7×1.6	7.69–7.98, 9.38–10.32	1.03,1.10	20	0.003	2	X band
[P]	10.6×10.3×1.6	7.2–18	2.5	15	0.002	1.9–5.1	C, X & Ku band

$$\beta_{ii} = 1 - \left(\sum_{j=1}^N |S_{ij}|^2 \right) \quad (16)$$

$$\beta_{ij} = -(S_{ii}^* S_{ij} + S_{ji}^* S_{ij}) \quad (17)$$

The diversity characteristics of a MIMO antenna system are discussed and contrasted with other reported literature as shown in Table 2. The volume of the presented antenna is $10.6 \times 10.3 \times 1.6 \text{ mm}^3$, which is very compact as compared to other MIMO antenna dimensions except [5–10], which are designed for a single element. Frequency ratio and ECC of the MIMO antenna are 2.5 and 0.002, respectively, which are good except [12]. The average isolation of the MIMO antenna is 15 dB, except [11–13, 15–17]. The proposed antenna achieves circular polarization from 7.2 GHz to 8.9 GHz frequency range, which does not consider other antennas as reported in Table 2 excluding [6, 17]. Thus, it may be summed up very well that the proposed dual element MIMO antenna has favourable traits to be utilized for C, X, and Ku band applications viably.

5. CONCLUSION

A dual-element circularly polarized MIMO antenna for C, X, and Ku bands with an isolation of 15 dB is designed, fabricated, and measured. The measured results demonstrate a decent likeness to simulated ones in the whole frequency range. The results demonstrate that the proposed structure operates from 7.2 to 18 GHz with good impedance matching. The antenna achieved an average peak gain and total efficiency of 2.21 dBi and 69.2%, respectively, with $\text{ECC} < 0.1607$ and $\text{CCL} < 0.35 \text{ bits/sec/Hz}$. It also offers high diversity gain 9.99 dB and satisfactory TARC $< -7 \text{ dB}$. Further, the capacity of MIMO antenna was also studied with the number of transmitting and receiving antenna elements. The performance of the suggested antenna has all the acceptable traits for MIMO systems.

REFERENCES

1. Rao, Q. and D. Wang, "A compact dual-port diversity antenna for long-term evolution handheld devices," *IEEE transactions on vehicular technology*, Vol. 59, No. 3, 1319–1329, 2009.
2. Kumar, A., S. K. Mahto, and R. Sinha, "Y-shaped antenna for 5g enabled gadgets and its mimo for smartphone applications," in *2020 URSI Regional Conference on Radio Science (URSI-RCRS)*, 1–4, IEEE, 2020.
3. Kumar, A., S. K. Mahto, R. Sinha, and A. Choubey, "Dual circular slot ring triple-band mimo antenna for 5g applications," *Frequenz*, Vol. 75, No. 3-4, 91–100, 2021.
4. Charola, S., S. K. Patel, J. Parmar, and R. Jadeja, "Multiband jerusalem cross-shaped angle insensitive metasurface absorber for x-band application," *Journal of Electromagnetic Waves and Applications*, 1–13, 2021.
5. Parikh, H., S. Pandey, and M. Sahoo, "Design of a modified E-shaped dual band patch antenna for Ku band application," *2012 International Conference on Communication Systems and Network Technologies*, 49–52, IEEE, 2012.
6. Thi, T. N., K. Hwang, and H. Kim, "Dual-band circularly-polarised spidron fractal microstrip patch antenna for ku-band satellite communication applications," *Electronics letters*, Vol. 49, No. 7, 444–445, 2013.
7. Sayed, A., R. Ghonam, and A. Zekry, "Design of a compact dual band microstrip antenna for ku-band applications," *International Journal of Computer Applications*, Vol. 115, No. 13, 2015.
8. Samsuzzaman, M., M. Islam, N. Misran, and M. M. Ali, "Dual band x shape microstrip patch antenna for satellite applications," *Procedia Technology*, Vol. 11, 1223–1228, 2013.
9. Vijayvergiya, P. L. and R. K. Panigrahi, "Single-layer single-patch dual band antenna for satellite applications," *IET Microwaves, Antennas & Propagation*, Vol. 11, No. 5, 664–669, 2016.
10. Saini, G. S. and R. Kumar, "A low profile patch antenna for ku-band applications," *International Journal of Electronics Letters*, 1–11, 2019.

11. El Ouahabi, M., A. Zakriti, M. Essaaidi, A. Dkiouak, and E. Hanae, "A miniaturized dual-band MIMO antenna with low mutual coupling for wireless applications," *Progress In Electromagnetics Research*, Vol. 93, 93–101, 2019.
12. Kumar, N., P. Kumar, and M. Sharma, "Superwideband dual notched band square monopole MIMO antenna for UWB/X/Ku band wireless applications," *2019 IEEE Indian Conference on Antennas and Propagation (InCAP)*, 1–5, IEEE, 2019.
13. Satam, V. and S. Nema, "Defected ground structure planar dual element MIMO antenna for wireless and short range radar application," *2015 IEEE International Conference on Signal Processing, Informatics, Communication and Energy Systems (SPICES)*, 1–5, IEEE, 2015.
14. Tan, C. M., M. R. Tripathy, et al., "A miniaturized T-shaped MIMO antenna for X-band and Ku-band applications with enhanced radiation efficiency," *2018 27th Wireless and Optical Communication Conference (WOCC)*, 1–5, IEEE, 2018.
15. Pouyanfar, N., C. Ghobadi, J. Nourinia, K. Pedram, and M. Majidzadeh, "A compact multi-band MIMO antenna with high isolation for C and X bands using defected ground structure," *Radioengineering*, Vol. 27, No. 3, 686–693, 2018.
16. Addepalli, T. and V. R. Anitha, "Compact two-port MIMO antenna with high isolation using parasitic reflectors for uwb, x and ku band applications," *Progress In Electromagnetics Research C*, Vol. 102, 63–77, 2020.
17. Eslami, A., J. Nourinia, C. Ghobadi, and M. Shokri, "Four-element MIMO antenna for X-band applications," *International Journal of Microwave and Wireless Technologies*, 1–8, 2021.
18. Singh, A. K., S. K. Mahto, and R. Sinha, "Compact super-wideband MIMO antenna with improved isolation for wireless communications," *Frequenz*, Vol. 75, No. 9-10, 407–417, 2021.
19. Glazunov, A. A., A. F. Molisch, and F. Tufvesson, "Mean effective gain of antennas in a wireless channel," *IET Microwaves, Antennas & Propagation*, Vol. 3, No. 2, 214–227, 2009.
20. Loyka, S. L., "Channel capacity of MIMO architecture using the exponential correlation matrix," *IEEE Communications letters*, Vol. 5, No. 9, 369–371, 2001.
21. Saxena, G., P. Jain, and Y. K. Awasthi, "High diversity gain super-wideband single band-notch MIMO antenna for multiple wireless applications," *IET Microwaves, Antennas & Propagation*, Vol. 14, No. 1, 109–119, 2019.